

# Calculations of Photoneutrons from Varian Clinac Accelerators and Their Transmissions in Materials\*

J. C. Liu<sup>1</sup>, K. R. Kase<sup>1</sup>, X. S. Mao<sup>1</sup>, W. R. Nelson<sup>1</sup>, J. H. Kleck<sup>2</sup>, and S. Johnson<sup>2</sup>

1) Stanford Linear Accelerator Center (SLAC), MS 48, P. O. Box 4349, Stanford, CA 94309, U.S.A.  
 (Fax 415-926-3569; e-mail: james@slac.stanford.edu)  
 2) Varian Associates, Inc., Palo Alto, CA 94304, U.S.A.

## Abstract

Monte Carlo calculations of the giant-dipole-resonance photoneutrons (GRN) around the Varian Clinac 2100C/2300C medical accelerator heads (10-20 MV modes) were made using the coupled EGS4-MORSE code. The actual head materials and geometries were simulated in great detail using the Combinatorial Geometry facility of MORSE. The neutron production (i.e., sites and yields) was calculated with EGS4 and, then, the neutron transport in the accelerator head was done with MORSE. Both the evaporation and direct neutron components of the GRN were considered by incorporating the EVAP4 code and an empirical algorithm, respectively, into MORSE. With the calculated neutron spectra around the head as source terms, MCNP4a was used to estimate the corresponding dose equivalent transmission (considering both the neutron attenuation and the build-up of captured gamma rays) in several different types of concrete. The calculated results of the absolute neutron fluence and spectra around the heads, as well as the transmission curves, are presented and discussed.

## Introduction

Electron linear accelerators used for medical radiation therapy, operated in bremsstrahlung mode above 10 MV, can produce neutrons through the photonuclear giant-dipole-resonance (GDR) reaction. Neutrons from the photon-induced GDR reaction consist of a large portion of evaporation neutrons which dominate at low neutron energies (< 1-2 MeV), and a small fraction of direct neutrons, which dominate at high energies. The reactions occur in the various materials in the Linac target, flattening filter, collimators, and movable jaws. The GDR photoneutrons then transport in and leak out of the accelerator head. Together with the leakage photons, these neutrons can pose significant shielding issues for linac radiotherapy facilities.

The EGS4 electron-photon Monte Carlo code [1] was used to calculate the photoneutron production in the Varian Clinac 2100C/2300C, operating in four bremsstrahlung modes at 10, 15, 18 and 20 MV. With the EGS4 photon history output file, a modified version of the MORSE neutron-photon code [2] was used to calculate the source neutron energy spectrum and the absolute leakage neutron fluence and spectra around the head. With the leakage neutron spectra as source terms, the MCNP4a code [3] with the ENDF/B-V continuous cross sections were used to calculate the corresponding dose equivalent transmission in commercially available concretes with different compositions and densities.

The calculations related to EGS4-MORSE have been reported in detail in four papers [4-7]. Therefore, only the major results in those works will be summarized below, and the main emphasis reported here is on the MCNP-related calculations.

## Methods and results

### 1. Neutron production and transport with EGS4-MORSE

Using the Combinatorial Geometry package of MORSE, an EGS4 user code was developed to simulate the complex geometry of the Linac head, as shown in Fig. 1. A photon history file was generated, which contained the parameters of position, direction, energy and track length for those photons capable of generating neutrons in each medium. These photon histories were then randomly sampled by MORSE. The total neutron yield (including both the evaporation and direct components) for the sampled photon was calculated by multiplying the corresponding photoneutron yield cross section [8] with the photon track length. The validity of the yield calculations has been shown by Mao et al. [5].

The fraction of the direct neutron yield was estimated using an empirical formula [6], developed from data by Mutchler [9]. A source neutron was then produced with a weight equal to the fractional yield (first evaporation, then direct) at a position randomly chosen along the length of the photon track.

The energies of the evaporation and direct neutrons were calculated using the EVAP4 code [10] and an empirical algorithm [6], respectively. Successful testing of this energy-determining method can be seen in the comparisons with measurements shown in Figs. 2 and 3 [6,11]. The angular distribution of the direct neutrons was assumed to be in the form of  $1+C\sin^2\theta$ , where  $\theta$  is the angle between the incoming photon and the emitted neutron and  $C$  is a constant dependent on neutron energy and the media isotope [6,9]. For neutrons with energies  $\leq 2.5$  MeV, the emissions are assumed to be isotropic, i.e.,  $C=0$ .

The EGS4-calculated neutron yields in the components of the head [5] with jaw fully closed, i.e., zero field size, are shown in Table 1. The primary collimators and the jaws (when closed) produce the majority of the neutrons (e.g., 99% at 10 MV). This is because of their close positions relative to primary bremsstrahlung beam, the tungsten's low GDR reaction threshold (6.2 MeV), and high GDR cross section. The neutron yield per unit photon dose (Gy) at the isocenter, as well as the relative yields, are also given. Reference 5 also shows the neutron yields for other field sizes. If we assume that all neutrons are produced near the target, without neutron absorption or multiplication in the head, the fluence at 1 m from the target can be estimated as the yield divided by  $4\pi(100)^2$  (see last row of Table 1).

Table 1. EGS4-calculated neutron yields in the Varian Clinac 2100C/2300C head (jaw closed).

Bremsstrahlung mode	20 MV	18 MV	15 MV	10 MV
Electron beam kinetic energy	22.3 MeV	18.8 MeV	14.9 MeV	10.3 MeV
Target	$3.8 \times 10^{-4}$ (W, Cu)	$1.9 \times 10^{-4}$ (W, Cu)	$4.1 \times 10^{-5}$ (W, Cu)	$1.7 \times 10^{-9}$ (Cu)
Primary collimators (tungsten)	$7.9 \times 10^{-4}$ (36%)	$4.9 \times 10^{-4}$ (40%)	$1.7 \times 10^{-4}$ (38%)	$5.9 \times 10^{-6}$ (44%)
Flattening filter	$2.3 \times 10^{-4}$ (Fe, Ta)	$1.1 \times 10^{-4}$ (Fe, Ta)	$1.0 \times 10^{-4}$ (W)	$4.5 \times 10^{-9}$ (Cu)
Jaws (tungsten)	$8.0 \times 10^{-4}$ (36%)	$4.2 \times 10^{-4}$ (34%)	$1.3 \times 10^{-4}$ (29%)	$7.3 \times 10^{-6}$ (55%)
Others (magnet, shielding, etc.)	$2.4 \times 10^{-5}$	$1.7 \times 10^{-5}$	$5.8 \times 10^{-6}$	$1.4 \times 10^{-7}$
Total yield per incident electron	$2.2 \times 10^{-3}$	$1.2 \times 10^{-3}$	$4.5 \times 10^{-4}$	$1.3 \times 10^{-5}$
Yield relative to 20 MV	1.0	0.55	0.20	0.006
Yield per dose (Gy) in isocenter	$1.2 \times 10^{12}$	$1.2 \times 10^{12}$	$6.8 \times 10^{11}$	$3.8 \times 10^{10}$
Yield relative to 20 MV	1.0	1.0	0.57	0.03
Fluence at 1 m ( $\text{cm}^{-2} \text{ Gy}^{-1}$ )	$9.5 \times 10^6$	$9.5 \times 10^6$	$5.4 \times 10^6$	$3.0 \times 10^5$

Figure 4 shows the seven positions around the head at which the neutron fluence and energy spectra were calculated [7] using the modified MORSE code described above. The corresponding fluence and average energy values are shown in Table 2. Positions 1 and 2 are in patient plane and positions 5 and 6 are symmetric about the head. The mean fluence, averaged over the 7 positions, at 1 m from the target is  $1.0 \times 10^7 \text{ cm}^{-2} \text{ Gy}^{-1}$  at 20 MV and decreases to  $2.2 \times 10^5 \text{ cm}^{-2} \text{ Gy}^{-1}$  at 10 MV. These mean fluence values are similar to the estimated fluences in Table 1. The mean energy of the leakage neutrons is 0.49, 0.44, 0.38 and 0.16 MeV at 20, 18, 15 and 10 MV, respectively. The mean ambient neutron dose equivalent [12] at 1 m from the target, H, per unit photon dose at the isocenter ranges from  $1.78 \text{ mSv Gy}^{-1}$  at 20 MV to  $0.02 \text{ mSv Gy}^{-1}$  at 10 MV. With a machine delivering a maximum photon dose rate up to  $6 \text{ Gy min}^{-1}$ , the neutron dose equivalent rate at 1 m can be as high as  $0.64 \text{ Sv h}^{-1}$ . With a workload of 500 Gy per week and a dose limit of  $1 \text{ mSv y}^{-1}$  outside the shielding (assumed 3 m away), a transmission factor of  $10^4$  is needed.

Table 2. Fluence  $\phi$  ( $\text{cm}^{-2} \text{ Gy}^{-1}$ ), average energy  $E_{\text{ave}}$ , and ambient dose equivalent  $H_n$  of the leakage neutrons around the Varian Clinac 2100C/2300C head (jaws closed), calculated with the modified MORSE code.

Position	20 MV		18 MV		15 MV		10 MV	
	$\phi$ ( $\times 10^7$ )	$E_{\text{ave}}$ (MeV)	$\phi$ ( $\times 10^7$ )	$E_{\text{ave}}$ (MeV)	$\phi$ ( $\times 10^6$ )	$E_{\text{ave}}$ (MeV)	$\phi$ ( $\times 10^5$ )	$E_{\text{ave}}$ (MeV)
1	1.2	0.47	1.1	0.43	5.4	0.39	3.0	0.16
2	0.39	0.49	0.33	0.46	1.9	0.42	0.87	0.17
3	0.50	0.40	0.47	0.38	2.5	0.35	1.2	0.14
4	0.49	0.46	0.45	0.47	2.1	0.32	0.75	0.16
5	1.2	0.58	1.2	0.48	6.0	0.39	2.4	0.17
6	1.3	0.57	1.2	0.50	5.9	0.41	2.4	0.17
7	1.4	0.40	1.2	0.38	6.1	0.33	3.5	0.15

Mean	1.0	0.49	0.9	0.44	4.7	0.38	2.2	0.16
$H_n$ (mSv Gy <sup>-1</sup> )		1.78		1.50		0.72		0.02

## 2. Neutron (and captured gammas) transmission in concretes calculated with MCNP4a

Figure 5 shows three neutron spectra at 20, 18 and 10 MV (mean of the two spectra at positions 5 and 6). The spectrum at 10 MV (average energy 0.17 MeV) has few neutrons above 1 MeV. The spectra at 20 MV and 18 MV represent the hardest and softest ones, respectively, of all leakage spectra around the head. They were used as source terms in MCNP4a to calculate the dose equivalent transmission in concrete ( $\rho = 2.35 \text{ g cm}^{-3}$  and 5% hydrogen by weight), Ledite XN288\* and Ledite XN240\*.

Figure 6 shows that the two different spectra at 20 and 10 MV have similar transmissions in concrete after the first two tenth value layer (TVL) thicknesses. The first TVL,  $T_1$ , is  $43 \text{ g cm}^{-2}$  and the equilibrium TVL,  $T_e$ , is  $79 \text{ g cm}^{-2}$ , both consistent with NCRP values [13]. The deep transmission is dominated by captured gammas (spectrum peaked at a few MeV), particularly for the softer neutron spectrum.

Figure 7 shows the transmissions of the leakage neutrons at the 20 MV mode for normal and heavy\* (XN-240, XN-288) concretes. Although the transmissions for the three materials are similar up to the second TVL thickness, a transmission factor of  $10^{-4}$ , for example, would be achieved by a thickness of 112 cm ( $263 \text{ g cm}^{-2}$ ) for normal concrete, 82 cm ( $316 \text{ g cm}^{-2}$ ) for XN-240, and 77 cm ( $356 \text{ g cm}^{-2}$ ) for XN-288. Because of the heavy metal in heavy concretes, the neutron component dominates at large thicknesses.

## Summary

Calculations of the GDR photoneutrons around the Varian Clinac 2100C/2300C Linac, as well as the related dose equivalent transmissions in normal and heavy concretes, have been made using a combination of EGS4-MORSE-MCNP4a. The maximum neutron output occurs at 20 MV, in which the mean fluence and ambient dose equivalent at 1 m from the beam target is  $10^7 \text{ cm}^{-2} \text{ Gy}^{-1}$  and  $1.78 \text{ mSv Gy}^{-1}$ , respectively., with an average energy of 0.49 MeV. The transmission in concrete does not depend heavily on the leakage neutron spectrum. On a per unit mass thickness basis, the AI heavy concretes provide less dose equivalent transmission (less neutron attenuation, but more captured gammas attenuation) than normal concrete.

## References

1. Nelson, W. R., Hirayama, H. and Rogers, D. W. O. *The EGS4 Code System*, Stanford Linear Accelerator Center, Stanford, CA, SLAC-265 (1985).
2. Emmett, M. B. *The MORSE Monte Carlo Radiation Transport Code System*, Radiation Shielding Information Center, Oak Ridge National Laboratory, Oak Ridge, TN, ORNL-4972 (1975).
3. Briesmeister, J. F. (ed.) *MCNP - A General Monte Carlo N-Particle Transport Code*. Version 4A, LA-12625-M, Los Alamos National Laboratory, New Mexico (1993).
4. Mao, X. S., Kase, K. R., Nelson, W. R. Giant dipole resonance neutron yields produced by electrons as a function of target material and thickness. *Health Phys.* 70:207-214 (1996).
5. Mao, X. S., Kase, K. R., Liu, J. C., Nelson, W. R., Kleck, J. H., and Johnson, S. Neutron sources in the Varian Clinac 2100C/2300C medical accelerator calculated by the EGS4 code. *Health Phys.* 72(4) (1997).
6. Liu, J. C., Nelson, W. R., Ken, K. R. and Mao, X. S. *Calculations of the Giant-Dipole-Resonance Photoneutrons Using a Coupled EGS4-MORSE Code*, Stanford Linear Accelerator Center, Stanford, CA, SLAC-PUB-95-6764 (1995) and also accepted for publication in Rad. Prot. Dosim. (1997).
7. Kase, K. R., Mao, X. S., Nelson, W. R., Liu, J. C., Kleck, J. H., and Johnson, S. Neutron fluence and energy spectra around the Varian Clinac 2100C/2300C medical accelerator. Stanford Linear Accelerator Center, Stanford, CA, SLAC-PUB-7190 (1996) and also submitted for publication in Health Physics.
8. Dietrich, S. S. and Berman, L. B. *Atlas of Photoneutron Cross Sections Obtained with Monoenergetic Photons*, At. Data Nucl. Data Tables, 38, 199 (1988).
9. Mutchler, G. S. *The Angular Distributions And Energy Spectra of Photoneutrons from Heavy Elements*, Ph.D. Thesis, Massachusetts Institute of Technology (1966).
10. ORNL, *EVAP Calculation of Particle Evaporation from Excited Compound Nuclei*. Radiation Shielding Information Center, Oak Ridge National Laboratory, Oak Ridge, TN, PSR-10 (1974).

\* Ledite XN288 and XN240 are heavy concrete products from Atomic International, Inc., Routes 73 & 663, P.O. Box 279, Frederick, PA 19435.

11. Liu, J. C., Rokni, S., Vylet, V., Arora, R., Semones, E., and Justus, A. Neutron Detection Time Distributions of Multisphere LiI Detectors and AB Remmeter at a 20-MeV Electron Linac. Stanford Linear Accelerator Center, Stanford, CA, SLAC-PUB-96-7353 (1996)
12. International Commission on Radiological Protection, Data for Use in Protection against External Radiation, ICRP Publication 51, Annals of the ICRP 17, No. 2/3, Pergamon Press, Oxford (1987).
13. National Council on Radiation Protection and Measurements, Neutron Contamination from Medical Electron Accelerators, NCRP Report 79, Bethesda, MD (1984).

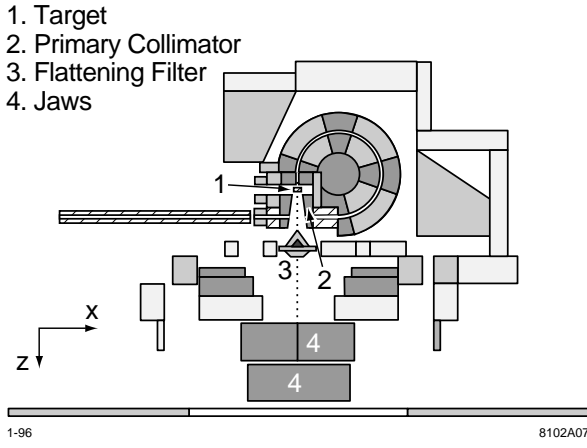


Figure 1. Combinatorial Geometry in the EGS4 simulation of the Varian Clinac 2100C/2300C accelerator head. The slice shows that the electron beam, after passing through the waveguide and the 270° bending magnet, hits the target (the two pairs of movable jaws are fully closed).

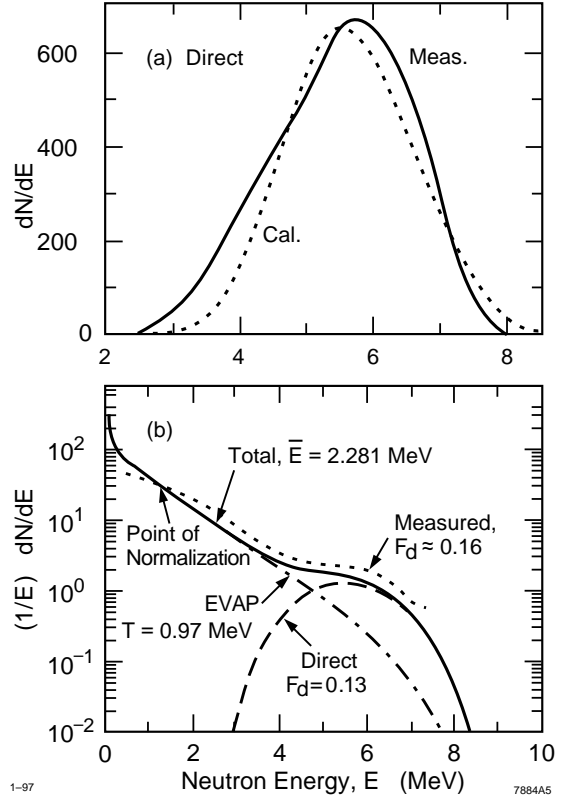


Figure 2. Spectral comparisons between the calculations and measurements [9] for direct neutrons (part a) and total neutrons (part b) from a lead target hit by quasi-monoenergetic 14 MeV photons. The nuclear temperature  $T$  for the evaporation neutrons is 0.97 MeV. The calculated fraction of direct neutron,  $F_d$ , is 0.13, 20% lower than the measurement of 0.16.

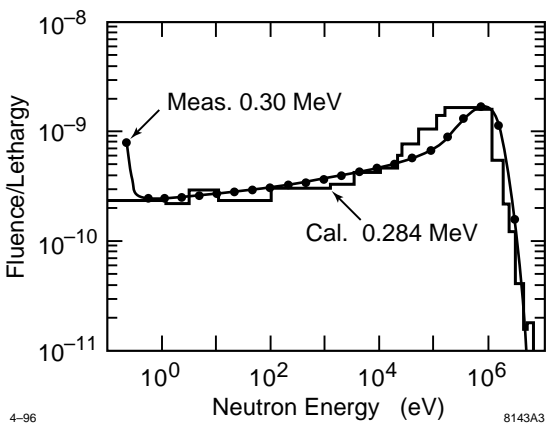


Figure 3. Comparison between the calculated neutron spectrum and multisphere measurements [11] from a copper target hit by 20-MeV electrons (average energy around 0.3 MeV).

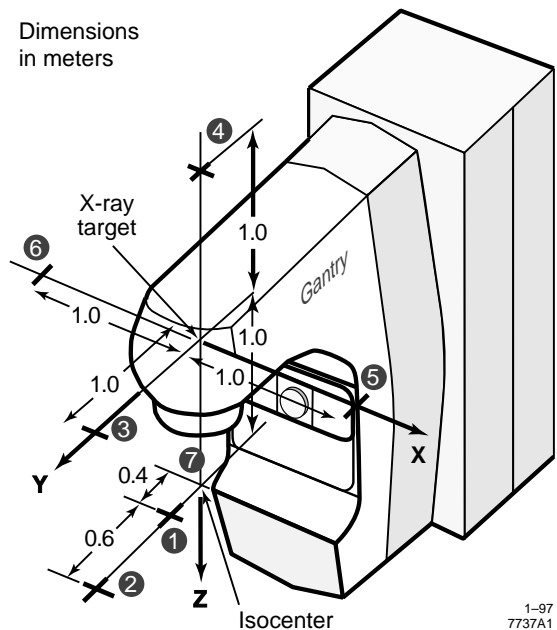


Figure 4. Locations at which neutron fluence and spectra were calculated with MORSE.

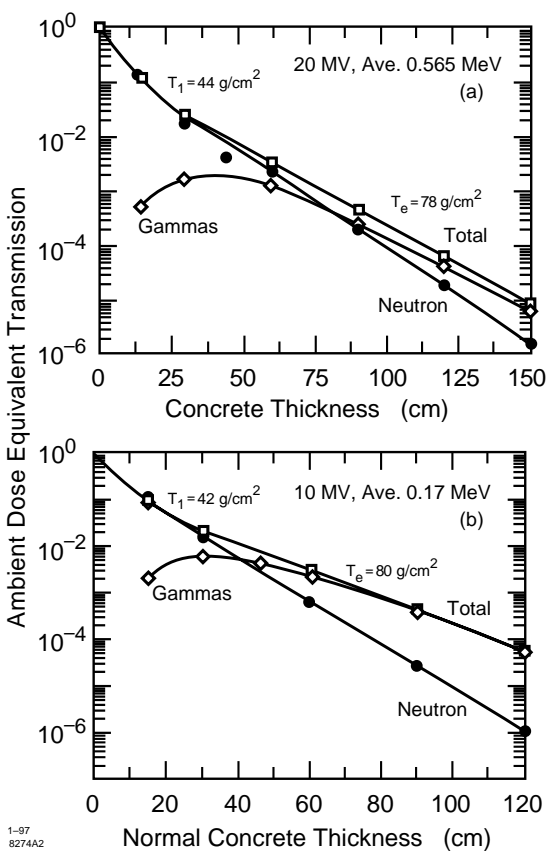


Figure 6. Relative transmission in concrete for two leakage neutron spectra in a broad parallel beam geometry. See text for detail.

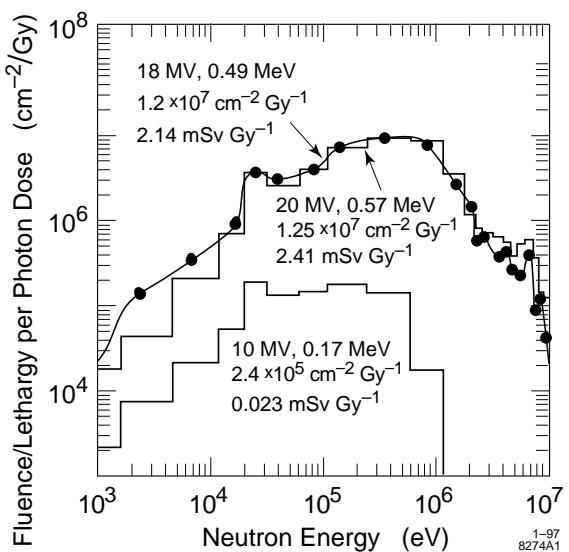


Figure 5. MORSE-calculated neutron spectra at 20, 18 and 10 MV (mean of two spectra at positions 5 and 6).

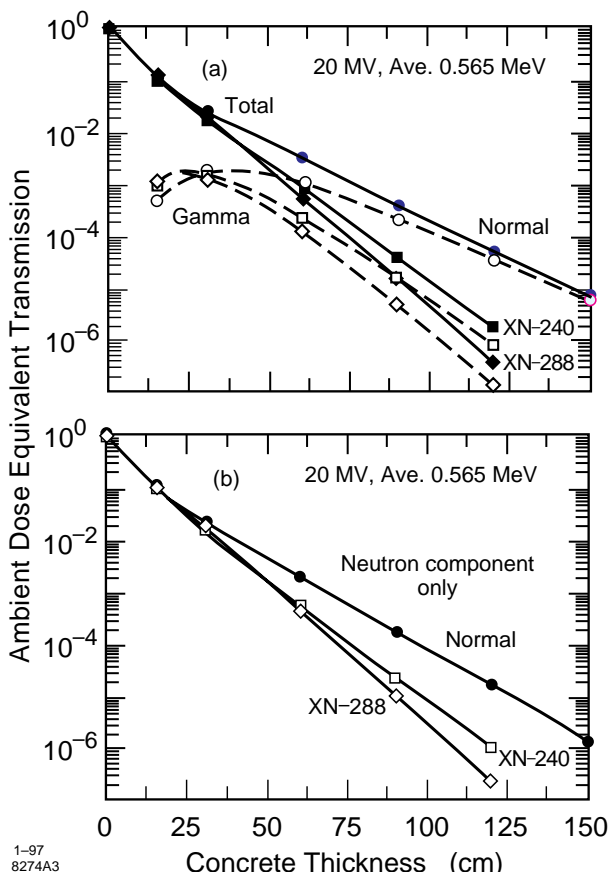


Figure 7. Relative transmission of the 20 MV leakage neutrons in normal and heavy concretes. See text for detail.